AD-A053 742   AIR FORCE MATERIALS LAB WRIGHT-PATTERSON AFB OHIO
SWELLING OF COMPOSITE LAMINATES.(U)
DEC 77   H T HAHN, R Y KIM   F/G 11/4

UNCLASSIFIED   AFML-TR-77-199   NL

| OF |
AD
A053742

END
DATE
FILMED
6-78
DDC

AFML-TR-77-199

SWELLING OF COMPOSITE LAMINATES

Mechanics & Surface Interactions Branch
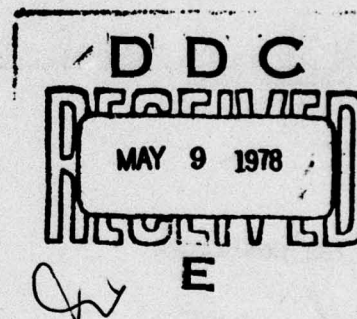Nonmetallic Materials Division

DDC

MAY 9 1978

E

December 1977

TECHNICAL REPORT AFML-TR-77-199

Final Report for Period September 1976 to September 1977

REPORT DOCUMENTATION PAGE		READ INSTRUCTIONS BEFORE COMPLETING FORM
1. REPORT NUMBER AFML-TR-77-199	**2. GOVT ACCESSION NO.**	**3. RECIPIENT'S CATALOG NUMBER**
4. TITLE (and Subtitle) SWELLING OF COMPOSITE LAMINATES		**5. TYPE OF REPORT & PERIOD COVERED** Final rept. 1 Sep 76 - 1 Sep 77
		6. PERFORMING ORG. REPORT NUMBER
7. AUTHOR(s) H. T. Hahn R. Y. Kim		**8. CONTRACT OR GRANT NUMBER(s)**
9. PERFORMING ORGANIZATION NAME AND ADDRESS Air Force Materials Laboratory (AFML/MBM) Air Force Wright Aeronautical Laboratories Wright-Patterson AFB, Ohio 45433		**10. PROGRAM ELEMENT, PROJECT, TASK AREA & WORK UNIT NUMBERS** 2037 2037P103
11. CONTROLLING OFFICE NAME AND ADDRESS Air Force Materials Laboratory (AFML/MBM) Air Force Wright Aeronautical Laboratories Wright-Patterson AFB, Ohio 45433		**12. REPORT DATE** Dec 77
		13. NUMBER OF PAGES 44
14. MONITORING AGENCY NAME & ADDRESS(if different from Controlling Office) WU AFML 2037 P 103 PE 64741F 2037 P1		**15. SECURITY CLASS. (of this report)** Unclassified
		15a. DECLASSIFICATION/DOWNGRADING SCHEDULE

16. DISTRIBUTION STATEMENT (of this Report)

Approved for public release; distribution unlimited.

17. DISTRIBUTION STATEMENT (of the abstract entered in Block 20, if different from Report)

18. SUPPLEMENTARY NOTES

19. KEY WORDS (Continue on reverse side if necessary and identify by block number)

Swelling	Absorption
Residual Stress	Desorption
Graphite/Epoxy	Hygrothermal Strain
Composite Materials	

20. ABSTRACT (Continue on reverse side if necessary and identify by block number)

The swelling behavior of a graphite/epoxy (AS/3501-5) is shown to be described by a model which is based on the assumption that the swelling is negligible until the moisture concentration reaches a threshhold value and then increases linearly thereafter. The model also provides a means of measuring the volume fraction of voids. The analytical results, which take into account the curing stresses, are compared with the experimental data for the transverse and thickness strains of symmetric laminates as well as for the warpage of unsymmetric laminates. The initial absorption in virgin specimens facilitates the subsequent

DD **FORM 1 JAN 73 1473** EDITION OF 1 NOV 65 IS OBSOLETE

diffusion and the residual stresses appear to be responsible for the absorption being slower than the desorption during the early stages of moisture conditioning. Warpage of unsymmetric laminates is discussed in light of the cracks found in constituent plies. Finally derived is a temperature-relative humidity relationship which renders the graphite/epoxy composite laminates free of residual stresses.

AFML-TR-77-199

FOREWORD

The work reported here was performed in the Mechanics and Surface Interactions Branch, Nonmetallic Materials Division, Air Force Materials Laboratory, Wright-Patterson AFB, Ohio. H. Thomas Hahn, AFML/MBM, was the principal investigator and R. Y. Kim of the University of Dayton Research Institute was responsible for the experimental phase of the project.

The authors wish to acknowledge R. Esterline and R. Cornwell for the preparation and testing of specimens. Sincere appreciation is extended to S. Dastin of the Grumman Aerospace Corporation for supplying some of the specimens tested.

```
ACCESSION for
NTIS          White Section  ☑
DDC           Buff Section   ☐
UNANNOUNCED                  ☐
JUSTIFICATION........................

.....................................
BY.................................
DISTRIBUTION/AVAILABILITY CODES
Dist.    AVAIL. and/or SPECIAL
A
```

iii

TABLE OF CONTENTS

LIST OF ILLUSTRATIONS

LIST OF ILLUSTRATIONS (CONTINUED)

LIST OF TABLES

SECTION I
INTRODUCTION

Susceptibility of polymers to swelling due to moisture absorption leads to the presence of residual stresses in the composite laminates which utilize such materials as matrix. In composite laminates a non-uniform moisture distribution is not the only cause of the swelling stress; even under a uniform distribution the residual stresses result from the incompatible swelling behavior between the matrix and fibers. The swelling stresses thus induced may lead to the creation of micro-cracks especially under transient conditions and further degrade the strength properties of composites. At the same time, however, these stresses generally negate the curing stresses and, hence, the combined effects may be beneficial. Thus, it is important to know not only the moisture diffusion behavior but also the swelling behavior, in order to properly characterize the material property change resulting from the moisture absorption.

Although the interfacial effects are not negligible, many of the moisture-related characteristics of composites are known to be traceable back to those of the matrix material. For example, moisture diffusion in graphite/epoxy composites is described by the Fick equation with a diffusion coefficient which can be predicted from the matrix properties (Reference 1). The matrix/interface-controlled properties degrade substantially at the high temperature wet conditions (Reference 2) and the glass transition temperature of composite is lowered similarly to that of matrix (Reference 3). The equilibrium swelling strains of composite and of matrix can be related to each other through a proper analysis (Reference 4).

In this report some experimental results for a graphite/epoxy composite (AS/3501-5) are presented to support the validity of the swelling strain model proposed in Reference 5. The model is basically derived from the result of a micromechanics analysis, but it can be modified slightly to accomodate the experimental observations. Both lamina and

laminate swelling strains are analyzed, and residual stresses calculated, by this model. A difference between the absorption and desorption rates is explained in terms of the residual stresses and stress dependency of diffusion. In addition, warpage of unsymmetric laminates is analyzed and the matrix cracking is discussed. Finally presented is a relation-ship between the temperature and the relative humidity which results in a residual stress-free state for the graphite/epoxy composite.

SECTION II

THEORETICAL BACKGROUND

1. HYGROTHERMAL STRAINS OF UNIDIRECTIONAL LAMINAE

It has been shown in Reference 5 that the swelling strains of a composite reinforced with moisture-insensitive fibers are given by

$$e_L^H = 0 , \quad e_T^H = \frac{1 + \nu_m}{3} s(c - c_v)H(c - c_v) \tag{1}$$

Here ν_m is the Poisson's ratio of matrix, s and c are the specific gravity and the moisture content, respectively, of the composite, and c_v represents the amount of moisture entrapped in the voids

$$c_v = v_v/s \tag{2}$$

where v_v is the void content. $H(\cdot)$ is the Heaviside step function.

In reality, the volume additivity, which has been assumed in the fore-going derivation, may not hold, but the swelling strain is still linearly related to the moisture concentration above a certain threshhold level. In this case Equation 1 can be generalized to

$$e_T^H = \alpha_T^H (c - c_v)H(c - c_v) \tag{3}$$

Equation 3 is graphically shown in Figure 1. Note that α_T^H is the transverse swelling coefficient to be determined experimentally and that c_v can now be regarded as a threshhold value of c below which no appreciable swelling occurs.

In the presence of temperature changes, the resultant nonmechanical strains of a unidirectional composite are given by

$$e_L = e_L^T + e_L^H , \quad e_T = e_T^T + e_T^H \tag{4}$$

If thermal expansion is linear with temperature change, then the thermal strains are

$$e_L^T = a_L^T \Delta T, \quad e_T^T = a_T^T \Delta T \tag{5}$$

In the subsequent analyses, the material behavior is assumed elastic and the swelling strains independent of temperature. For convenience, the thermal strains are measured in the dry state as the temperature is changed from the initial stress-free reference to the final temperature and then the swelling strains are superimposed at the final temperature.

4
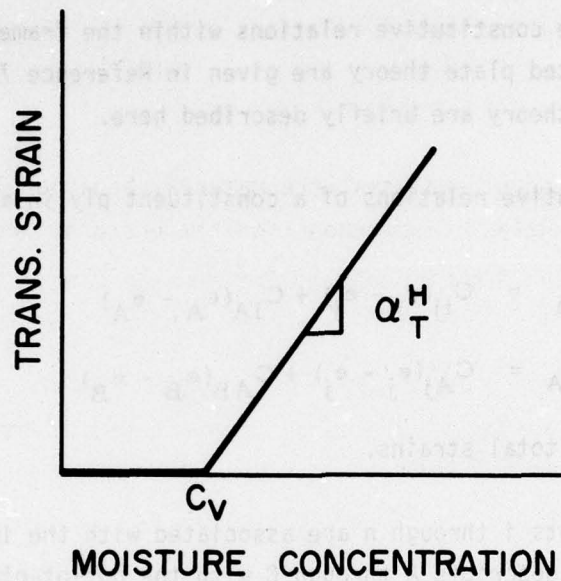
Figure 1. Analytical Model for Swelling Strain

2. HYGROTHERMAL STRAINS OF MULTIDIRECTIONAL LAMINATES

The laminate constitutive relations within the framework of the classical laminated plate theory are given in Reference 7. The salient features of the theory are briefly described here.

The constitutive relations of a constituent ply in a laminate can be written as

$$\sigma_i = C_{ij}(e_j - e_j) + C_{iA}(e_A - e_A) \tag{6}$$

$$\sigma_A = C_{Aj}(e_j - e_j) + C_{AB}(e_B - e_B) \tag{7}$$

where ε_i are the total strains.

The subscripts i through n are associated with the in-plane coordinates and the subscripts A through C with the out-of-plane coordinates. C's are the stiffnesses at the final state of interest.

According to the classical laminated plate theory, σ_A are assumed to be constant through the thickness and the total strains ε_i are given by

$$e_i = e_i^o + k_i z \tag{8}$$

where k_i are the curvatures and z is the thickness coordinate. Therefore, introducing the reduced stiffnesses Q_{ij}

$$Q_{ij} = C_{ij} - C_{iA} C_{AB}^{-1} C_{Bj} \tag{9}$$

one can derive the laminate constitutive relations as

$$N_i = A_{ij} e_j^o + B_{ij} k_j - N_i^N + T_{iB} \sigma_B \tag{10}$$

$$M_i = B_{ij} e_j^o + D_{ij} k_j - M_i^N + R_{iB} \sigma_B \tag{11}$$

$$\overline{e_A} = \overline{C_{AB}^{-1} \sigma_B} - \overline{C_{AB}^{-1} C_{Bj}} \; e_j^o - \overline{C_{AB}^{-1} C_{Bj} z} \; k_j$$

$$+ \overline{C_{AB}^{-1} C_{Bj} e_j} + \overline{e_A} \tag{12}$$

Here A_{ij}, B_{ij}, and D_{ij} are the usual laminate stiffnesses, and N_i^N and M_i^N are the nonmechanical forces and moments, respectively. An over bar stands for the average through the thickness h,

$$\overline{(\ )} = \frac{1}{h} \int_{-h/2}^{h/2} (\ )dz \tag{13}$$

and

$$[T_{iB}, R_{iB}] = \int_{-h/2}^{h/2} C_{iA} C_{AB}^{-1} [1, z]dz \tag{14}$$

The nonmechanical laminate strains ε_i^{oN} and curvatures k_i^N are obtained by putting $N_i = M_i = \sigma_B = 0$ in Equations 10 through 12:

$$e_i^{oN} = F_{ij}^{-1}(N_j^N - B_{ik}D_{kn}^{-1}M_n^N) \tag{15}$$

$$k_i^N = D_{ij}^{-1}(M_j^N - B_{jk}e_k^{oN}) \tag{16}$$

$$\overline{e}_A^N = \overline{e}_A + \overline{C_{AB}^{-1}C_{Bj}e_j} - \overline{C_{AB}^{-1}C_{Bj}}\ e_j^{oN} \tag{17}$$

$$- \overline{C_{AB}^{-1}C_{Bj}z}\ k_j^N$$

where

$$F_{ij} = A_{ij} - B_{ik}D_{kn}^{-1}B_{nj} \tag{18}$$

The in-plane residual stresses in each ply are then obtained from Equation 6 with the aid of Equation 9:

$$\sigma_i^R = Q_{ij}(e_j^{oN} + k_j^N z - e_j) \tag{19}$$

Moisture diffusion in composite laminates has been shown to be described fairly well by the Fick equation (Reference 1). The solution to this equation for a thin laminate undergoing moisture absorption or

7

desorption from an equilibrium state is well known (for example, see Reference 8). The expressions for the moisture concentration c and the average moisture content through the thickness, $\overline{c}$, are repeated here for convenience:

$$\frac{c - c_0}{c_\infty - c_0} = 1 - \frac{4}{\pi} \sum_{j=0}^{\infty} \frac{(-1)^j}{(2j + 1)} \cos \frac{(2j + 1)\pi z}{h} \exp\left(- \frac{(2j + 1)^2 \pi^2 Dt}{h^2}\right) \quad (20)$$

$$\frac{\overline{c} - c_0}{c_\infty - c_0} = 1 - \frac{8}{\pi^2} \sum_{j=0}^{\infty} \frac{1}{(2j + 1)^2} \exp\left(- \frac{(2j + 1)^2 \pi^2 Dt}{h^2}\right) \quad (21)$$

Here D is the diffusivity, t the time, and the subscripts 0 and ∞ stand for the initial and the final equilibrium state, respectively. Note that $\overline{c}_\infty = c_\infty$ and $\overline{c}_0 = c_0$.

The through-the-thickness distribution of the unconstrained swelling strain follows upon substitution of Equation 20 into Equation 1 or 3, in general. The final laminate strains and curvatures due to swelling are then obtained by solving Equations 15 through 18.

For symmetric laminates the nonmechanical moments M_i^H vanish because c is also symmetrically distributed with respect to the mid-plane. Furthermore, since c depends on z/h and also since the nondimensional time Dt/h^2 can be expressed in terms of $\overline{c}$ from Equation 21, the laminate swelling strains can be shown to depend only on the average moisture content independently of the thickness and diffusivity. Thus, all laminates of the layup $[\theta_{n_1}^{(1)} / \theta_{n_2}^{(2)} / \theta_{n_3}^{(3)} / \text{---}]_s$ will follow the same

relationship between the swelling strains, both in-plane and out-of-plane, and the average moisture content $\overline{c}$, as long as the ply ratio $n_1 : n_2 : n_3 : \text{---}$ remains the same. Since the relationship is independent of the diffusivity, so it is of the temperature insofar as the equilibrium moisture content remains the same. The aforementioned result is useful in that the

swelling strains of symmetric laminates can be determined within the shortest time by testing the thinnest possible laminate at the highest allowable temperature.

For unidirectional laminae, Equation 15 for the swelling strain reduces to

$$\epsilon_T^{oH} = a_T^H \frac{1}{h} \int_{-h/2}^{h/2} (c - c_v)H(c - c_v)dz \tag{22}$$

or

$$\epsilon_T^{oH} = a_T^H \gamma \bar{c} \tag{23}$$

where γ is the fraction of the moisture content that contributes to swelling. If the moisture profile through the thickness is as shown in Figure 2, then γ is the shaded area divided by the total area under the moisture profile.

In an absorption test it is possible that $c \geq c_v$ everywhere. In this case Equation 23 reduces to

$$\epsilon_T^{oH} = a_T^H (\bar{c} - \bar{c}_v) \text{ if } \bar{c} \geq \bar{c}_v \tag{24}$$

where $\bar{c}_v$ is the value of $\bar{c}$ when c reaches c_v everywhere. Thus the swelling coefficient and the threshhold value c_v can be determined from the linear region of the plot of ϵ_T^{oH} versus $\bar{c}$. However, the same is not true for the desorption test. The relationship between $\bar{c}_v$ and c_v is shown in Figure 3.
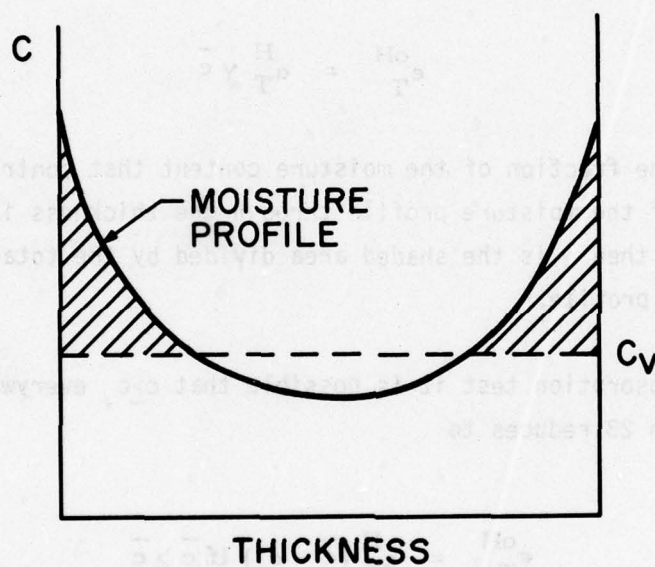
9

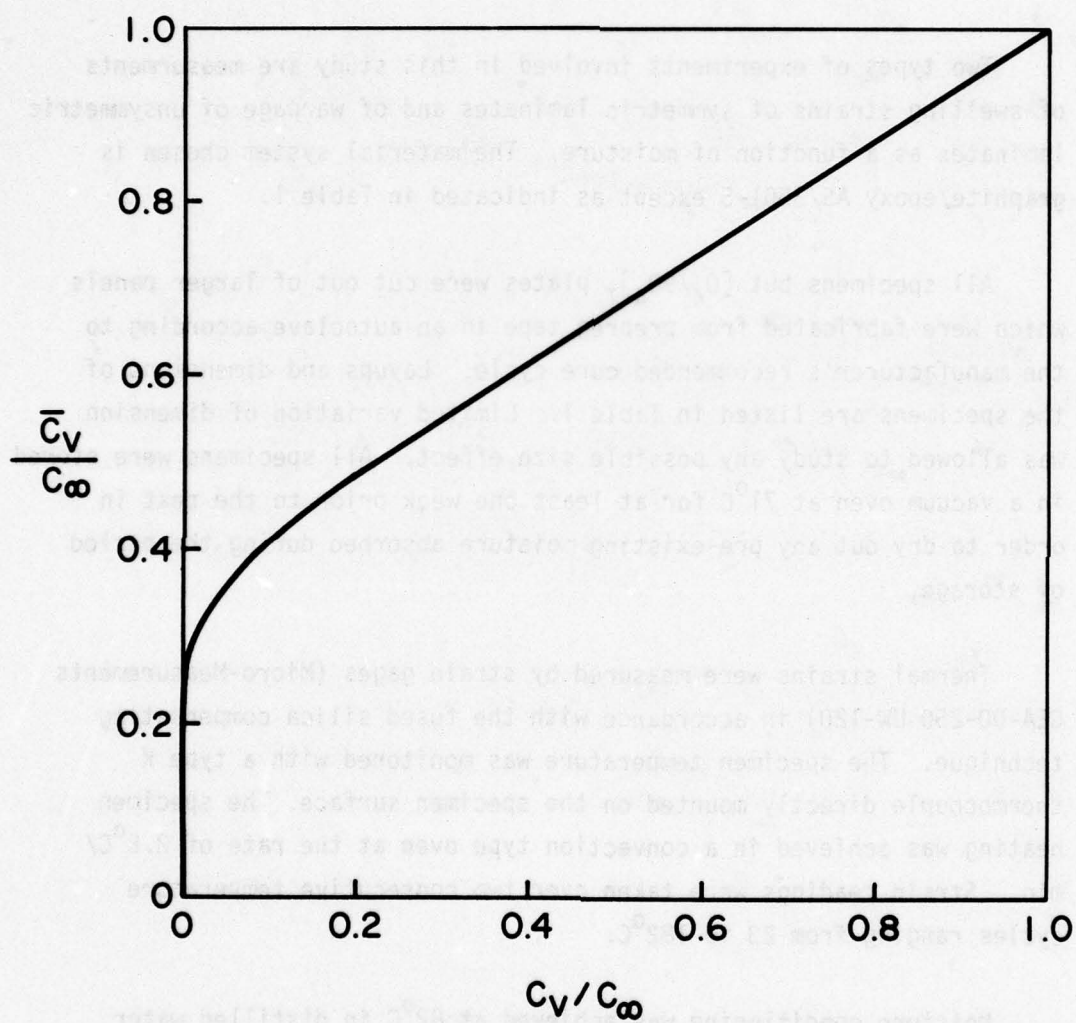Figure 2. Fraction of Moisture Content Which Contributes to Swelling

Figure 3. Relationship Between $\bar{c}_v$ and c_v

SECTION III

EXPERIMENTAL CORRELATION

1. EXPERIMENTAL PROCEDURE

Two types of experiments involved in this study are measurments
of swelling strains of symmetric laminates and of warpage of unsymmetric
laminates as a function of moisture. The material system chosen is
graphite/epoxy AS/3501-5 except as indicated in Table 1.

All specimens but $[0_4/90_4]_T$ plates were cut out of larger panels
which were fabricated from prepreg tape in an autoclave according to
the manufacturer's recommended cure cycle. Layups and dimensions of
the specimens are listed in Table 1. Limited variation of dimension
was allowed to study any possible size effect. All specimens were stored
in a vacuum oven at 71^oC for at least one week prior to the test in
order to dry out any pre-existing moisture absorbed during the period
of storage.

Thermal strains were measured by strain gages (Micro-Measurements
CEA-00-250 UW-120) in accordance with the fused silica compensating
technique. The specimen temperature was monitored with a type K
thermocouple directly mounted on the specimen surface. The specimen
heating was achieved in a convection type oven at the rate of $2.8^oC/$
min. Strain readings were taken over two consecutive temperature
cycles ranging from 23 to 182^oC.

Moisture conditioning was achieved at 82^oC in distilled water
for absorption and in vacuum for desorption. The time interval be-
tween the first and second conditioning was about six months and the
data were analyzed independently for each cycle.

12

TABLE 1.
SPECIMEN DIMENSIONS

Type of Test	Laminate	Specimen Number	Dimension, mm (Width x Length)
Thermal Expansion	$[0]_{8T}$	0 – 3	76 x 76
Swelling (Width)	$[0]_{8T}$	0 – 1	19 x 25
		0 – 2	76 x 76
Swelling (Thickness)	$[0]_{8T}$	0 – 1	19 x 25
		0 – 2	76 x 76
	$[0/90_3]_s$	B – 1	19 x 25
		B – 2	76 x 76
Deflection	$[0_4/90_4]_T$	US – 1 through 7	76 x 76
		UF – 1 through 7	76 x 76

Swelling strains were measured by either a micrometer of gage length 2.54 cm or a caliper of gage length 20.3 cm. The resolutions of the micrometer and the caliper are 0.00254 and 0.0127 mm, respectively. Strain measurements were taken at four locations for the thickness expansion and at three locations for the transverse and axial directions. The longitudinal strain of unidirectional lamina and the in-plane strains of multidirectional laminates are not reported, since they are negligibly small.

The unsymmetric plates, supplied by the Grumman Aerospace Corp., were fabricated under two different cure processes: a cooldown rate of 0.55°C/min to 121°C followed by a post cure of 3 hrs at $187.8 \pm 5.6^{\circ}$C for the specimens US-1 through 7, and a cooldown rate of 2.8°C/min followed by a post cure of 8 hrs at $176.7 \pm 5.6^{\circ}$C for the specimens UF-1 through 7.

The plates were initially warped due to the residual curing stresses. The deflection, defined as the relative displacement of the center of the plate when placed on a flat surface, was monitored as a function of moisture content by a travelling telescope with resolution of 0.01 mm. The same moisture conditioning as in the case of in-plane strain measurements was employed and the tests were terminated when the deflection nearly vanished.

2. RESULTS AND DISCUSSION

The transverse swelling strains obtained from the unidirectional specimens are shown in Figure 4. During absorption both specimens exhibit almost the same behavior independently of the test sequence. The threshhold value $\overline{c}_v$ above which the swelling strain increases linearly with the moisture content is seen to be approximately 0.9 percent. The slope of this linear portion is the swelling coefficient α_T^H and the intersection of its extension with the abscissa yields c_v:

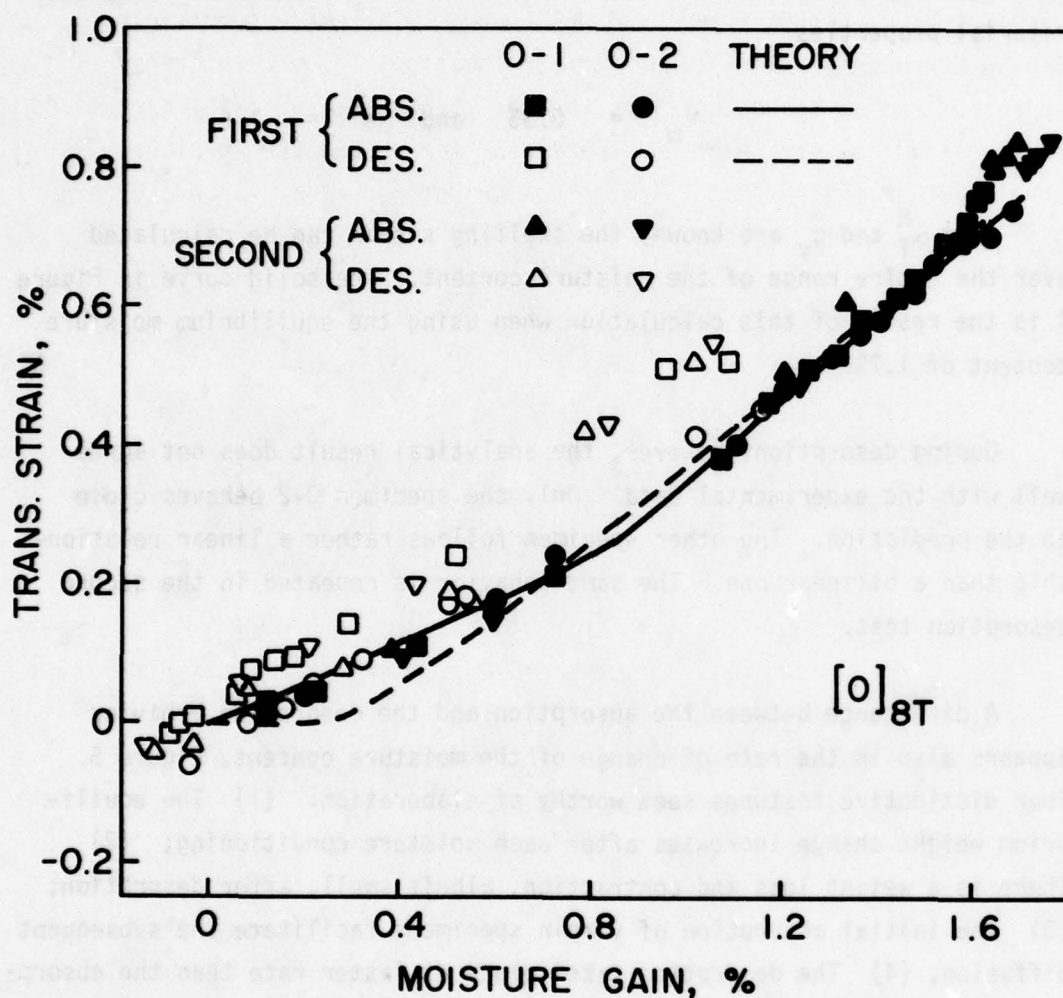$$\alpha_T^H = 0.59 \text{ and } c_v = 0.4\%$$

14

Figure 4. Transverse Swelling Strain of $[0]_{8T}$ Laminate

It is interesting to note that the measured swelling coefficient is lower than the theoretical value of 0.72 that follows from Equation 1 and the material properties

$$\nu_m = 0.35 \quad \text{and} \quad s = 1.6$$

Once α_T^H and c_v are known, the swelling strain can be calculated over the entire range of the moisture content. The solid curve in Figure 4 is the result of this calculation when using the equilibrium moisture content of 1.7%.

During desorption, however, the analytical result does not agree well with the experimental data. Only the specimen 0-2 behaves close to the prediction. The other specimen follows rather a linear relationship than a bilinear one. The same behavior is repeated in the second desorption test.

A difference between the absorption and the desorption behavior appears also in the rate of change of the moisture content, Figure 5. Four distinctive features seem worthy of elaboration: (1) The equilibrium weight change increases after each moisture conditioning; (2) There is a weight loss and contraction, albeit small, after desorption; (3) The initial absorption of virgin specimens facilitate the subsequent diffusion; (4) The desorption takes place at faster rate than the absorption. Furthermore, the linear portion of the weight change versus (time)$^{1/2}$ relationship is longer in absorption than in desorption.

The first two observations indicate the possibilities of microvoid formation and of leaching out of low molecular weight material (Reference 9). The third points toward the additional possibility of microcracking during the first cycle which may open up the passageway for the subsequent moisture diffusion but do not necessarily entrap moisture. The last observation as well as the poor experimental correlation in Figure 4 can be explained in terms of the residual stresses due to swelling as follows.
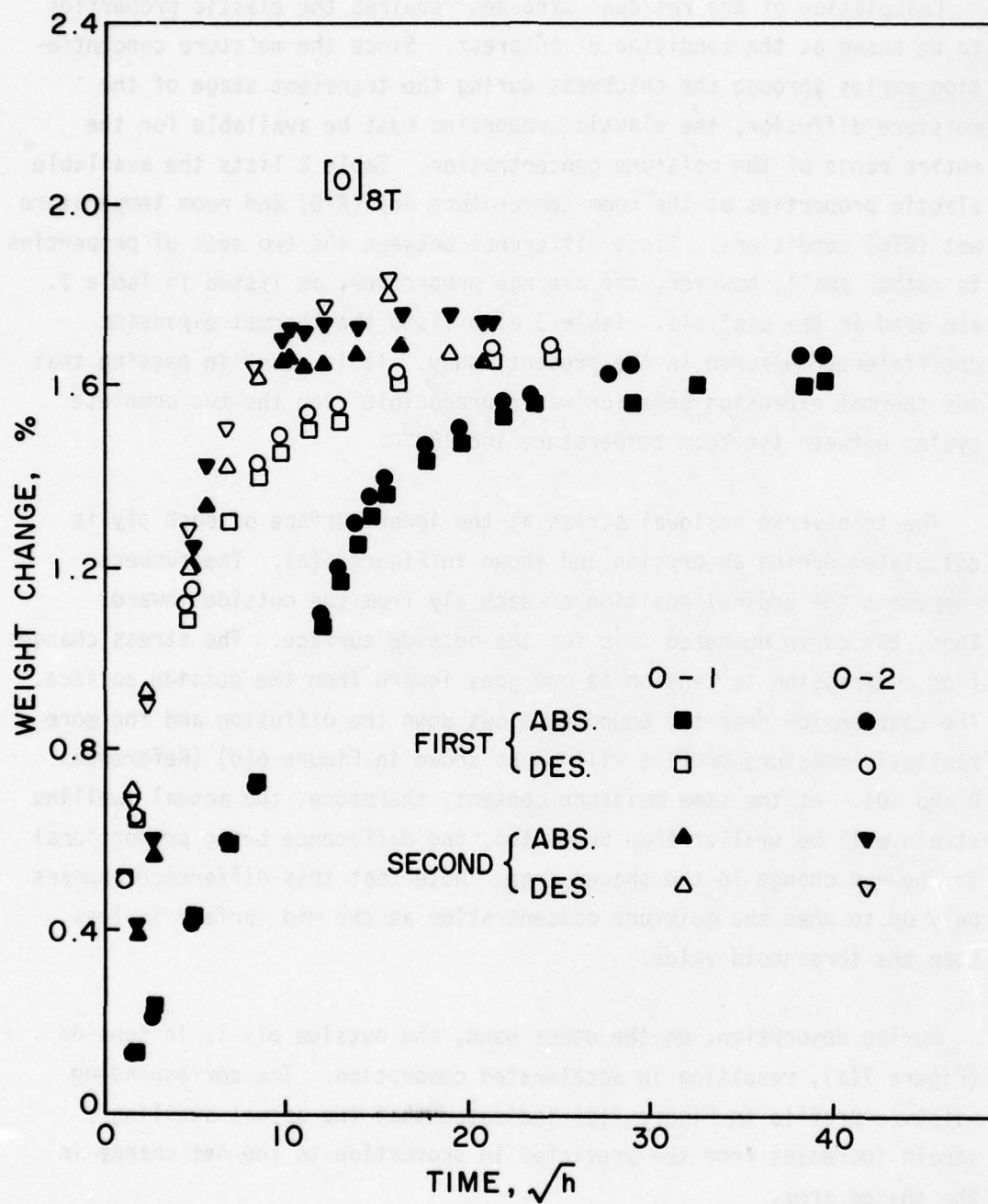
16

Figure 5. Weight Change Versus (time)$^{1/2}$ for $[0]_{8T}$ Laminates

Calculation of the residual stresses requires the elastic properties to be known at the condition of interest. Since the moisture concentration varies through the thickness during the transient stage of the moisture diffusion, the elastic properties must be available for the entire range of the moisture concentration. Table 2 lists the available elastic properties at the room temperature dry (RTD) and room temperature wet (RTW) conditions. Since difference between the two sets of properties is rather small, however, the average properties, as listed in Table 3, are used in the analysis. Table 3 also lists the thermal expansion coefficients measured in the present study. It is noted in passing that the thermal expansion behavior was reproducible over the two complete cycles between the room temperature and 182°C.

The transverse residual stress at the lower surface of each ply is calculated during absorption and shown in Figure 6(a). The numbers represent the ordinal position of each ply from the outside inward. Thus, the curve numbered 1 is for the outside surface. The stress changes from compression to tension as one goes inward from the outside surface. The compression near the boundary slows down the diffusion and the more realistic moisture profile will be as shown in Figure 6(b) (References 8 and 10). At the same moisture content, therefore, the actual swelling strain will be smaller than predicted, the difference being proportional to the net change in the shaded area. Note that this difference appears only up to when the moisture concentration at the mid surface is less than the threshhold value.

During desorption, on the other hand, the outside ply is in tension (Figure 7(a), resulting in accelerated desorption. The corresponding moisture profile in Figure 7(b) indicates that the actual swelling strain increases from the predicted in proportion to the net change in the shaded area.

Although the transverse stress at the outside surface exceeds the transverse strength, no visible cracks were detected by microscopic examinations of up to x300 magnification. The reason may be because only a small region is subjected to the high tensile stress while the rest are in compression.

TABLE 2

RT TENSILE PROPERTIES

	E_L GPa	ν_{LT}	E_T GPa	G_{LT} GPa	ν_{TT}[a]	X_T[b] MPa
Dry	138	0.30	9.65	4.21	0.33	48
Wet	132	0.34	8.62	3.76	0.33	32

a. Estimated

b. Transverse strength in tension

TABLE 3

AVERAGE PLY PROPERTIES

E_L GPa	ν_{LT}	E_T GPa	G_{LT} GPa	ν_{TT}	Thickness mm
135	0.32	9.14	3.99	0.33	0.14

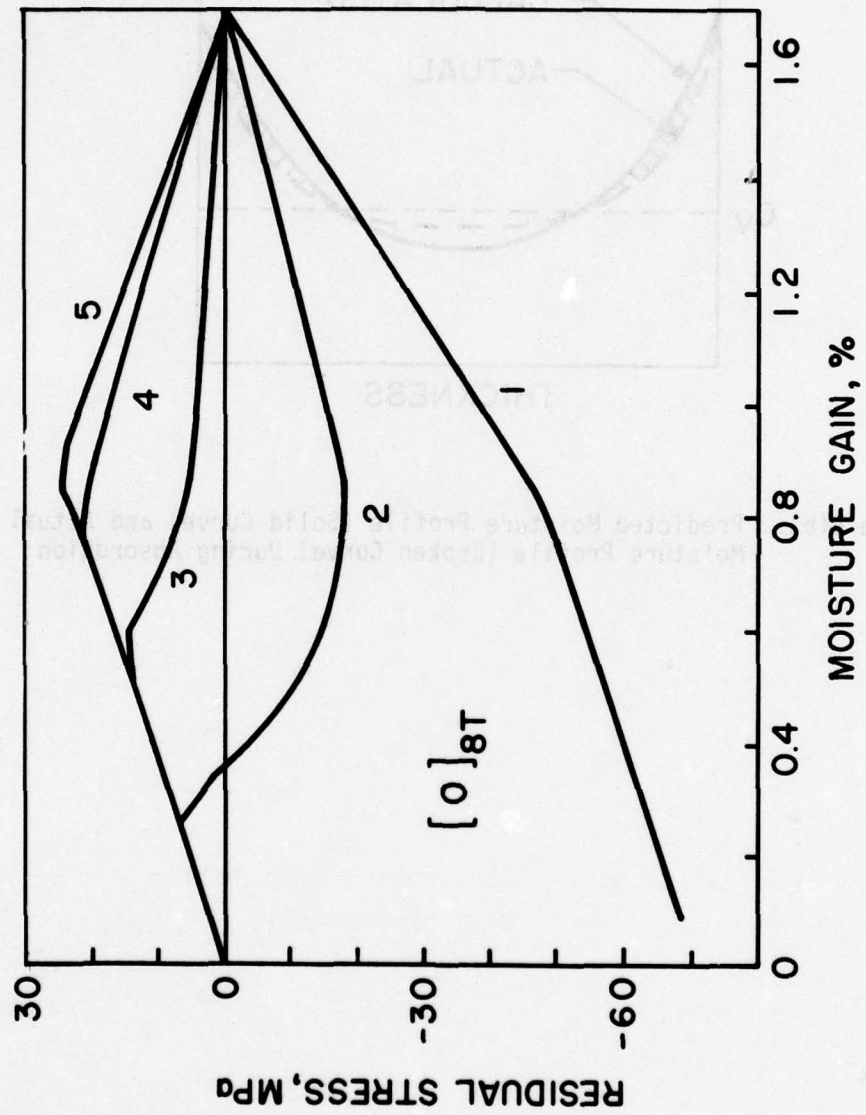| α_L^T μm/m/°K	α_T^T μm/m/°K	α_L^H	α_T^H
-0.3	28.1	0	0.59

20

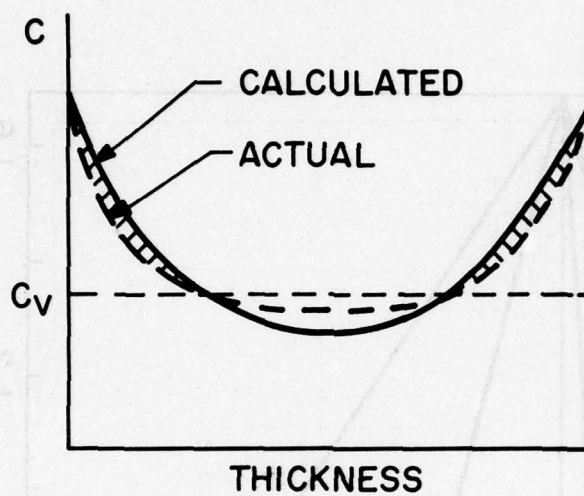Figure 6(a). Transverse Residual Stresses in $[0]_{8T}$ Laminate During Moisture Absorption

Figure 6(b). Predicted Moisture Profile (Solid Curve) and Actual
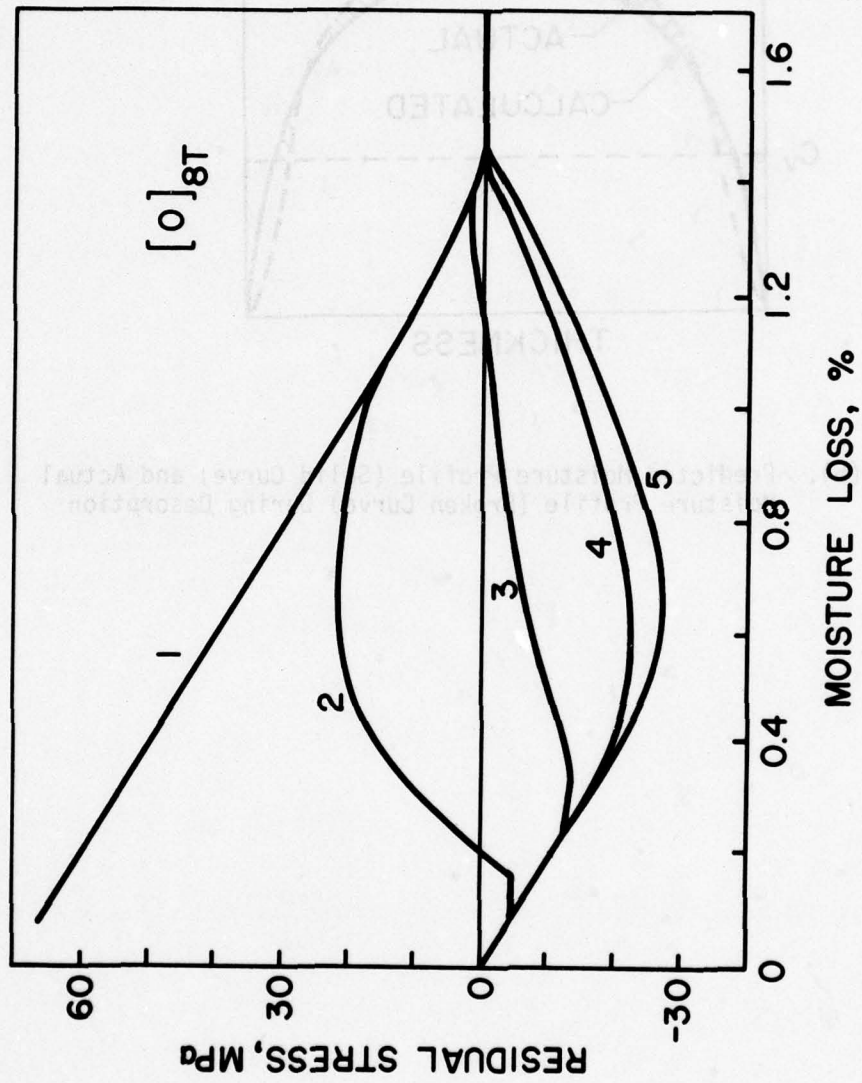Moisture Profile (Broken Curve) During Absorption

Figure 7(a). Transverse Residual Stresses in [0]$_{8T}$ Laminate During Moisture Desorption
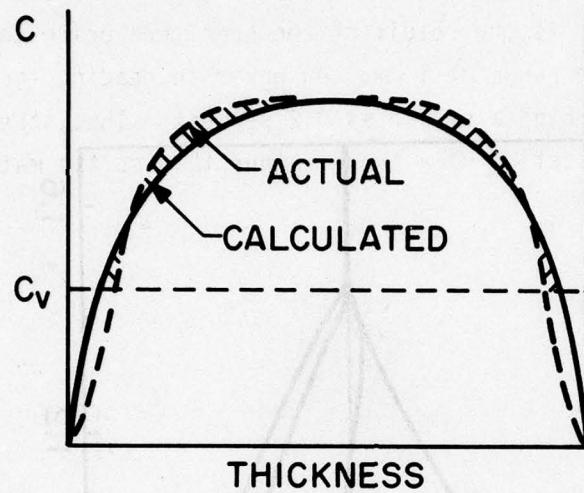
Figure 7(b). Predicted Moisture Profile (Solid Curve) and Actual Moisture Profile (Broken Curve) During Desorption

The thickness strains of the $[0]_{8T}$ and $[0/90_3]_s$ laminates are shown in Figures 8(a) and 8(b), respectively. For the $[0]_{8T}$ laminate, the analytical result is the same as that for the transverse strain. Large scatter in the data is the result of the specimens being too thin; the thickness is in the range of 1 mm. An error in reading the micrometer can add or subtract as high a strain as 0.2 percent. Thus, the data should be taken as an indication of a trend rather than as the material property itself.

The absorption and desorption behavior of the $[0/90_3]_s$ laminate is very similar to that of the $[0]_{8T}$ laminate, Figure 9. The initially tensile, transverse residual stresses in the inside plies, which result from the cure, become compressive as the moisture concentration increases in these plies, Figure 10(a). In Figure 10(a) the letters L and U stand for the lower and the upper surface, respectively. During desorption the outside surface is subject to a tensile transverse stress which remains comparable to the curing stress independently of the moisture loss, Figure 10(b).

The warpage of the square $[0_4/90_4]_T$ laminate is calculated from k_i^N by using the equation

$$\left| w^N \right|_{max} = \frac{1}{2}\left(\frac{a}{2}\right)^2 k_1^N \quad , \quad k_i^N = k_i^T + k_i^H$$

where a is the length of one side. Both analytical and experimental results are shown in Figure 11. The warpage is not exactly symmetric on both sides and only the maximum values, except at the dry state, are given for the reasons described later. The initial warpage is due to the curing stress and its prediction is based on the thermoelastic properties in Table 3.

The data in Figure 11 indicates that the specimen US-5 exhibits more warpage than the UF-5. To check if this is generally representative of the difference between US and UF specimens, warpage measurements were taken on other specimens and the results are listed in Table 4.

25

TABLE 4

DEFLECTION AT ROOM TEMPERATURE AND NUMBER OF CRACKS

Specimen No.	Deflection, mm		No. of Cracks		Remarks
	0-deg Ply Down	90-deg Ply Down	0-deg Ply	90-deg Ply	
US-1	1.75	0.90	0	11	a
UF-1	1.37	1.00	4	1	a
US-2	1.52	1.20	0	8	a
UF-2	1.18	1.08	3	6	a
US-4	Not measured		1	11	b
UF-4			4	1	b
US-5	Not measured		1	11	c
UF-5	1.00	1.60	6	0	c
US-6	2.40	0.75	1	9	d
UF-6	1.35	1.55	4	2	d
US-7	1.82	0.88	1	13	e
UF-7	1.35	1.22	4	15	e

a. Specimens were heated to 150°C.
b. Specimens were kept in water at 82°C for one year.
c., d. Specimens were used in the swelling tests.
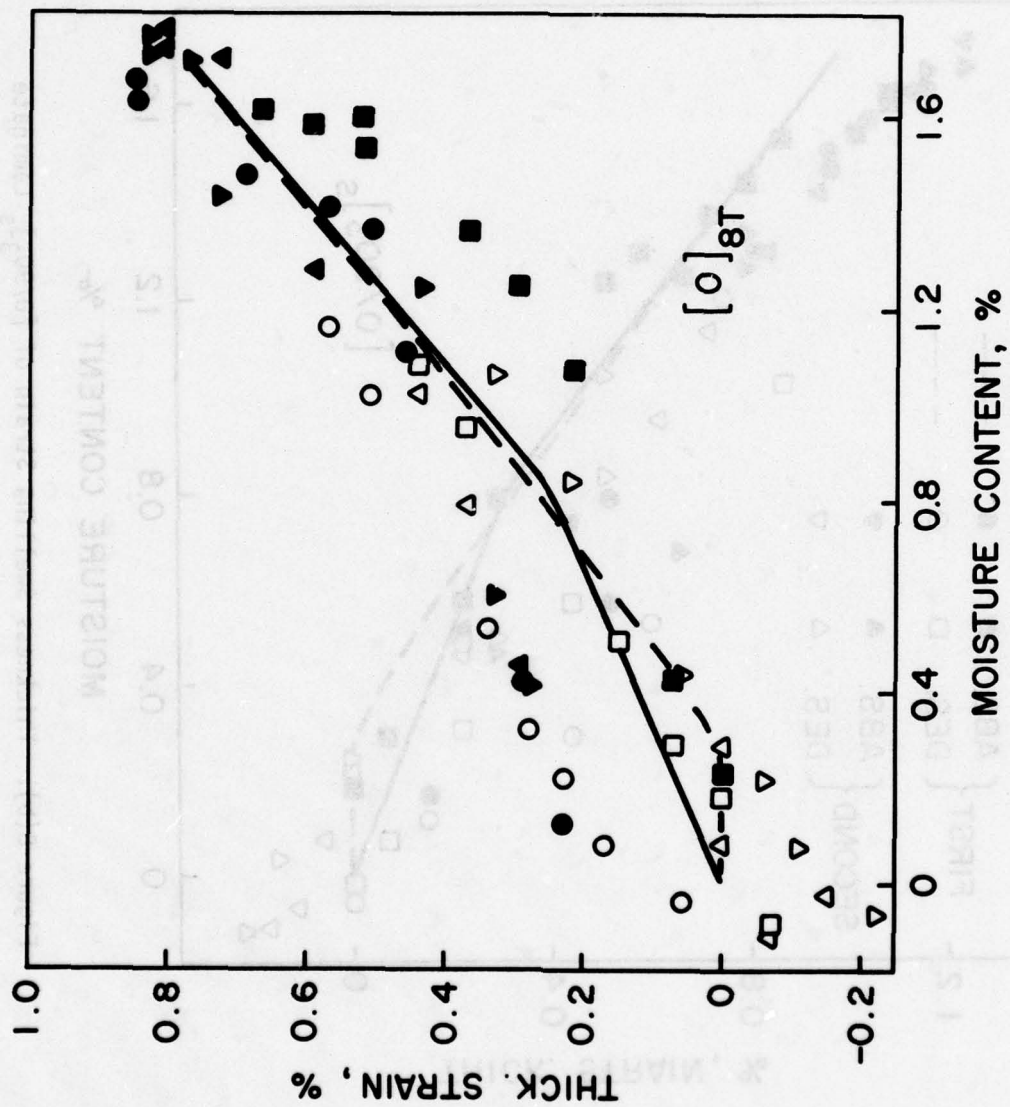d. Deflections were measured in the dry state.
e. No test was done.

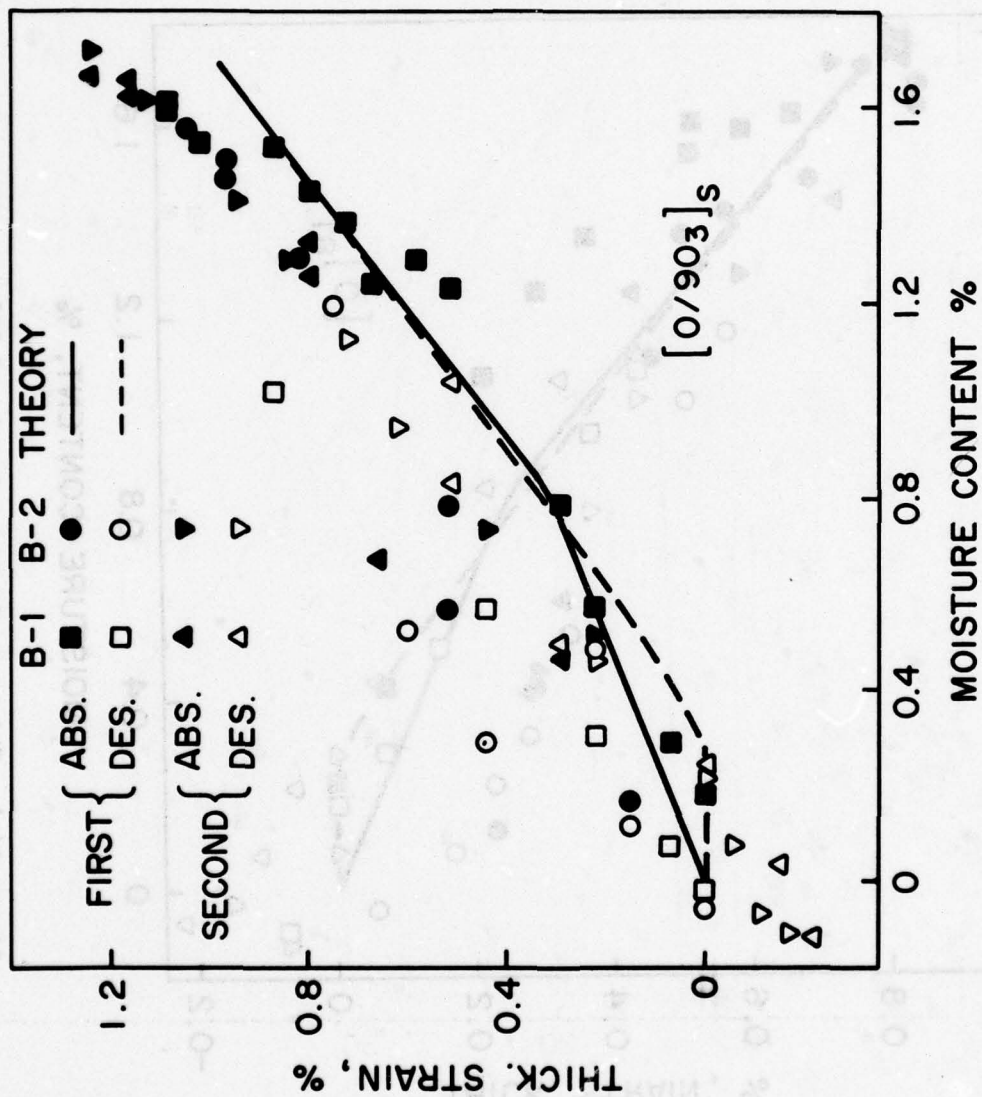Figure 8(a). Thickness Swelling Strain of $[0]_{8T}$ Laminate

Figure 8(b). Thickness Swelling Strain of $[0/90_3]_s$ Laminate
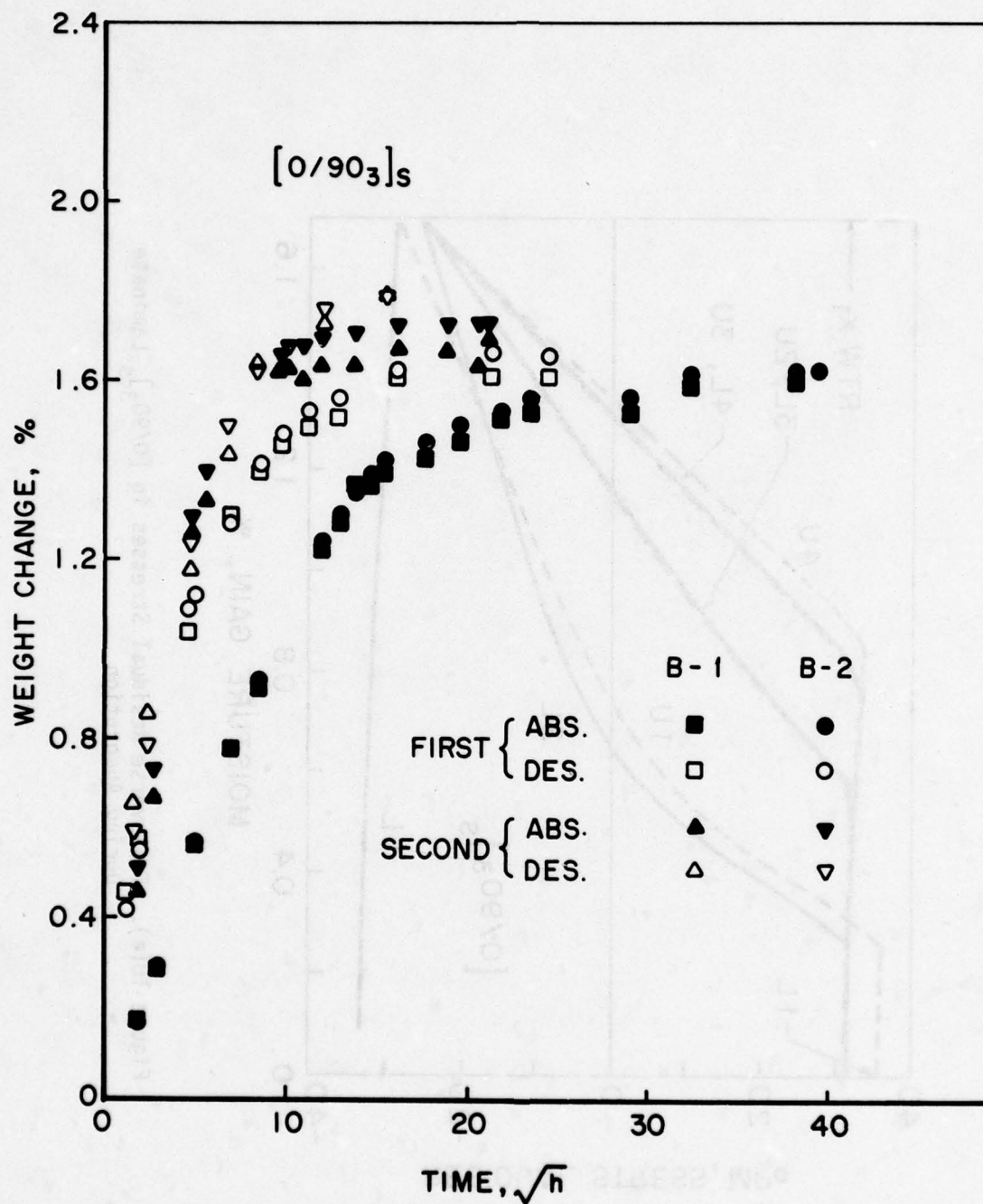
28

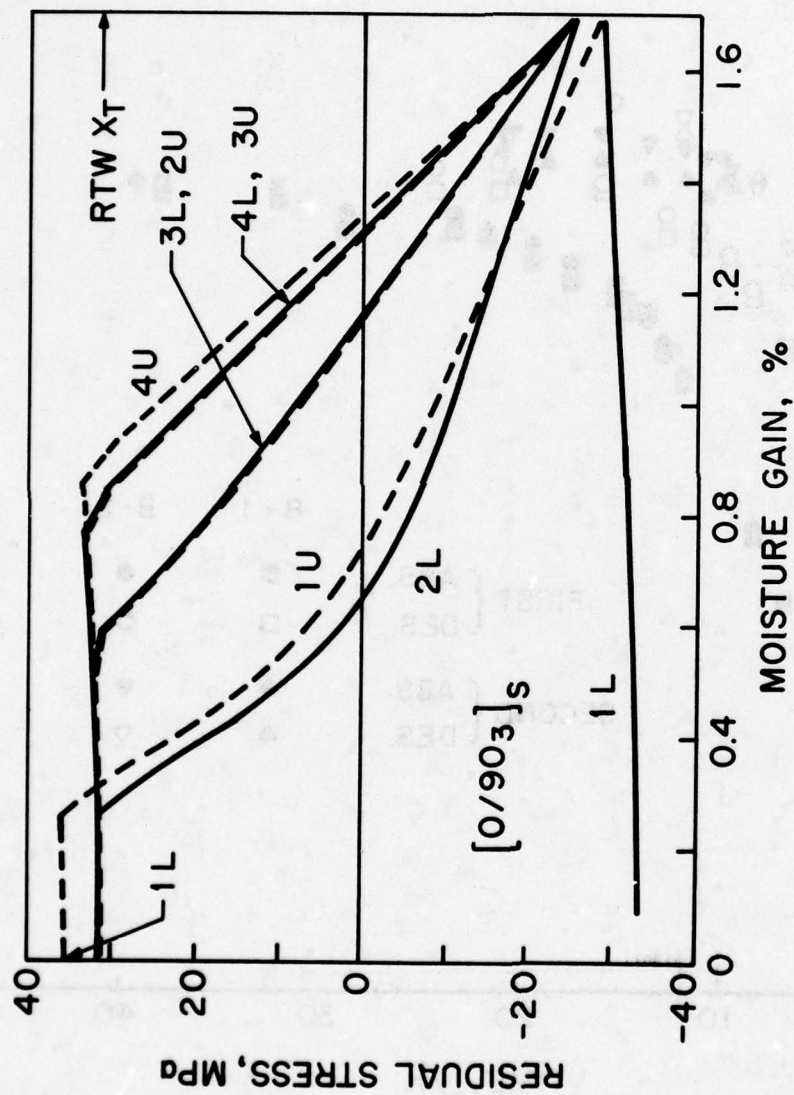Figure 9. Weight Change Versus (time)$^{1/2}$ for [0/90$_3$]$_s$ Laminates

Figure 10(a). Transverse Residual Stresses in $[0/90_3]_s$ Laminate During Absorption
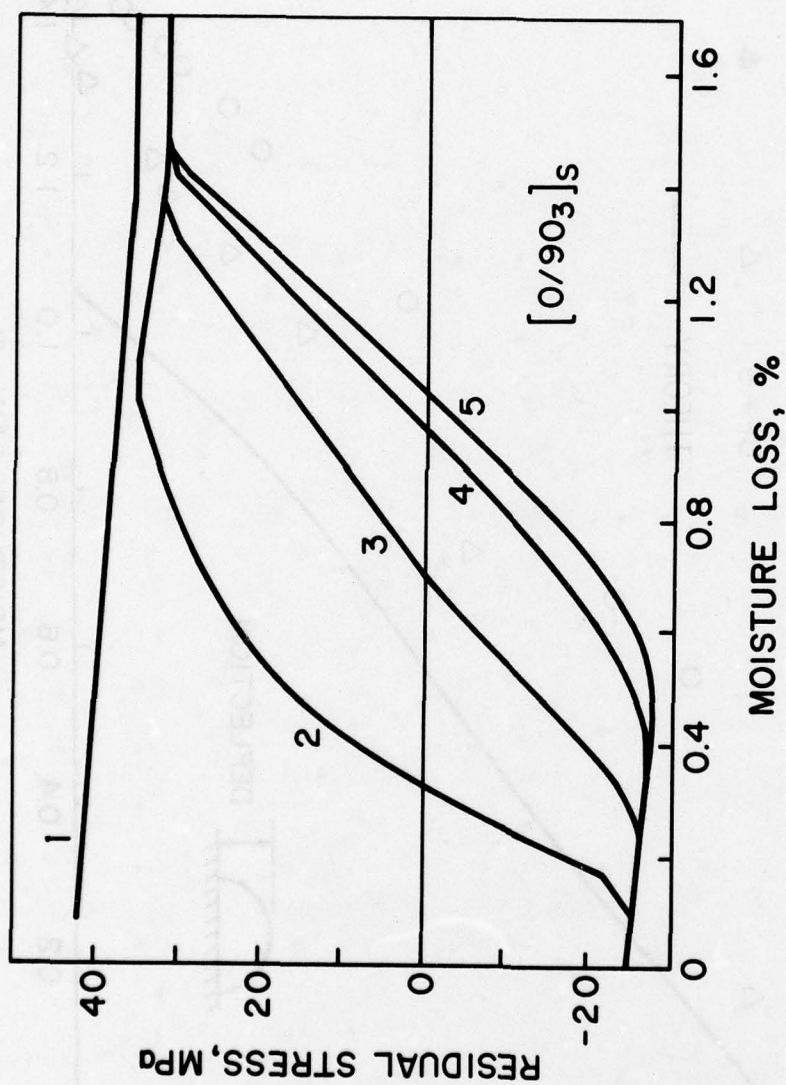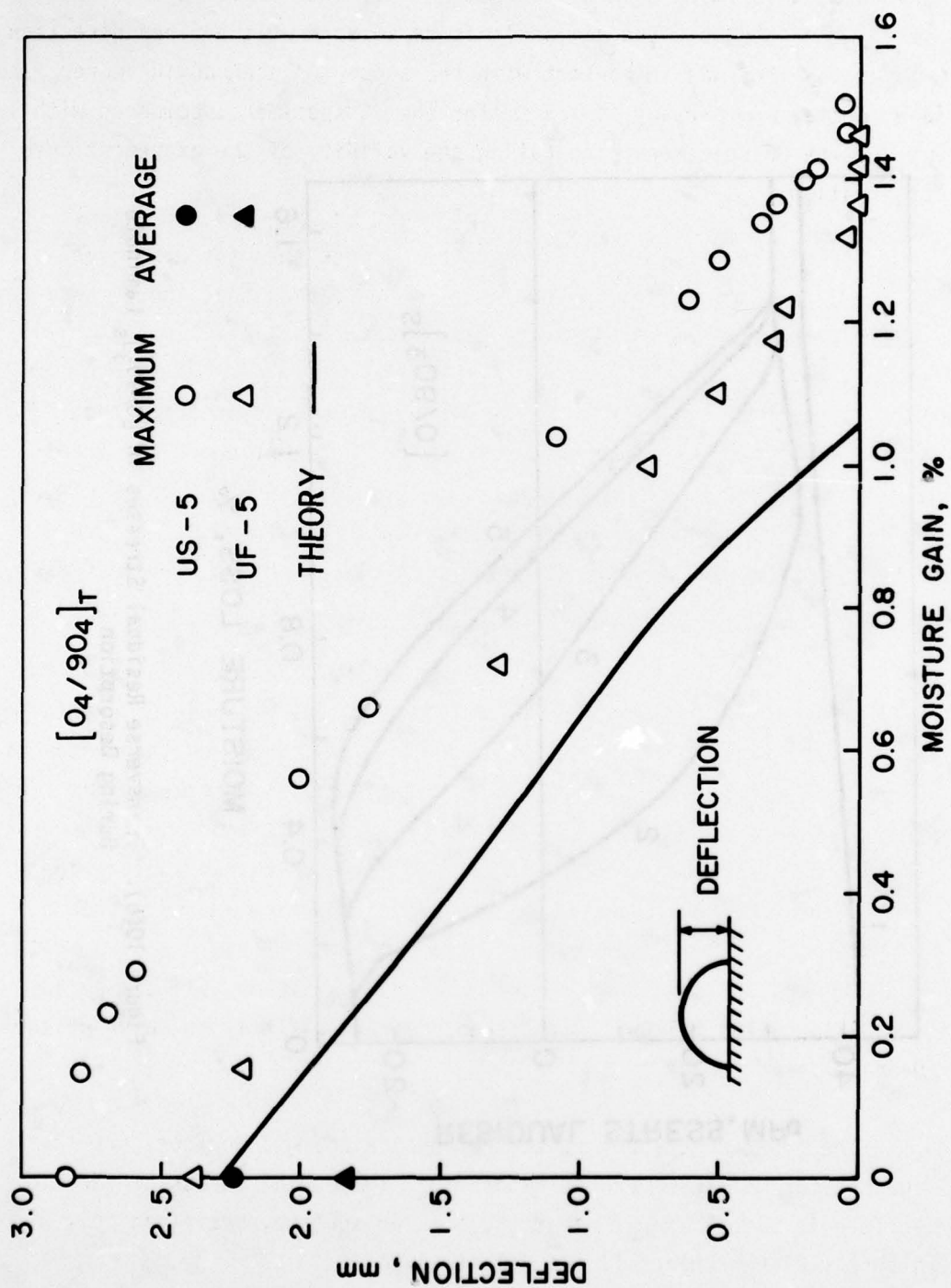
Figure 10(b). Transverse Residual Stresses in $[0/90_3]_s$ Laminate During Desorption

Figure 11. Deflection of $[0_4/90_4]_T$ Laminate During Absorption

All specimens except those numbered 4 and 6 had been kept in the room environment for more than a year and are believed to be in an equilibrium state. In the table the ply angle is measured from the fiber direction of the ply that was in contact with the support platen during cure. The average maximum warpage is 1.7 mm for the US specimens, compared with 1.3 mm for the UF specimens, indicating the validity of the aforementioned observation.

The measured warpage is seen to be greater than the predicted. However, the slopes are almost the same, indicating that the discrepancy is due rather to the cure than to the swelling.

To determine the cause of the warpage being unsymmetric, each specimen was polished on two perpendicular, adjacent edges and transverse cracks were located and counted. Examination of a few specimens on two parallel, opposite edges revealed that most cracks found were through the entire specimen width. A typical crack is shown in Figure 12.

Comparison of the warpage with the number of cracks in Table 4 indicates that the less contraction is due to the presence of cracks except for the specimen UF-1. The warpage resulting from the contraction of the plies with fewer cracks is larger for the US specimens than for the UF specimens. This is in line with the observation that the average number of cracks in the US specimens (10) is higher than that in the UF specimens (7) since both conditions, more warpage and more cracks, are indicative of higher residual stress. For some reasons unknown the US specimens invariably have more cracks in the 90-deg plies, whereas the UF specimens follow a rather random trend slightly in favor of the 0-deg plies.

The transverse stresses at the outside and mid surfaces are plotted against the moisture gain in Figure 13. The curing stress at the mid surface is higher than that at the outside surface, but it is only slightly higher than half the RTD strength.
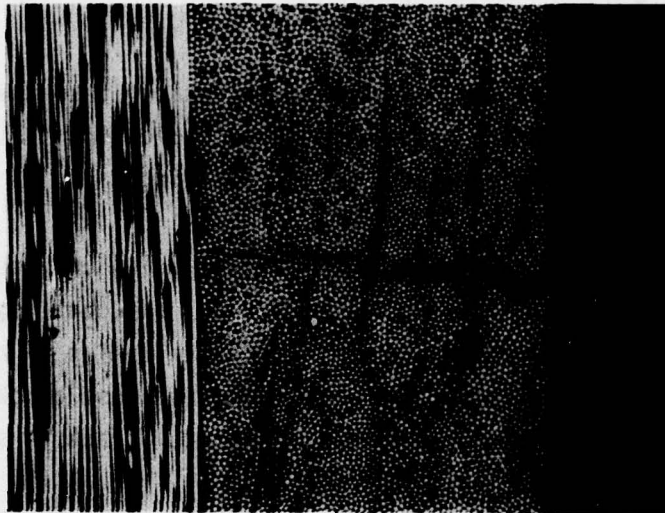
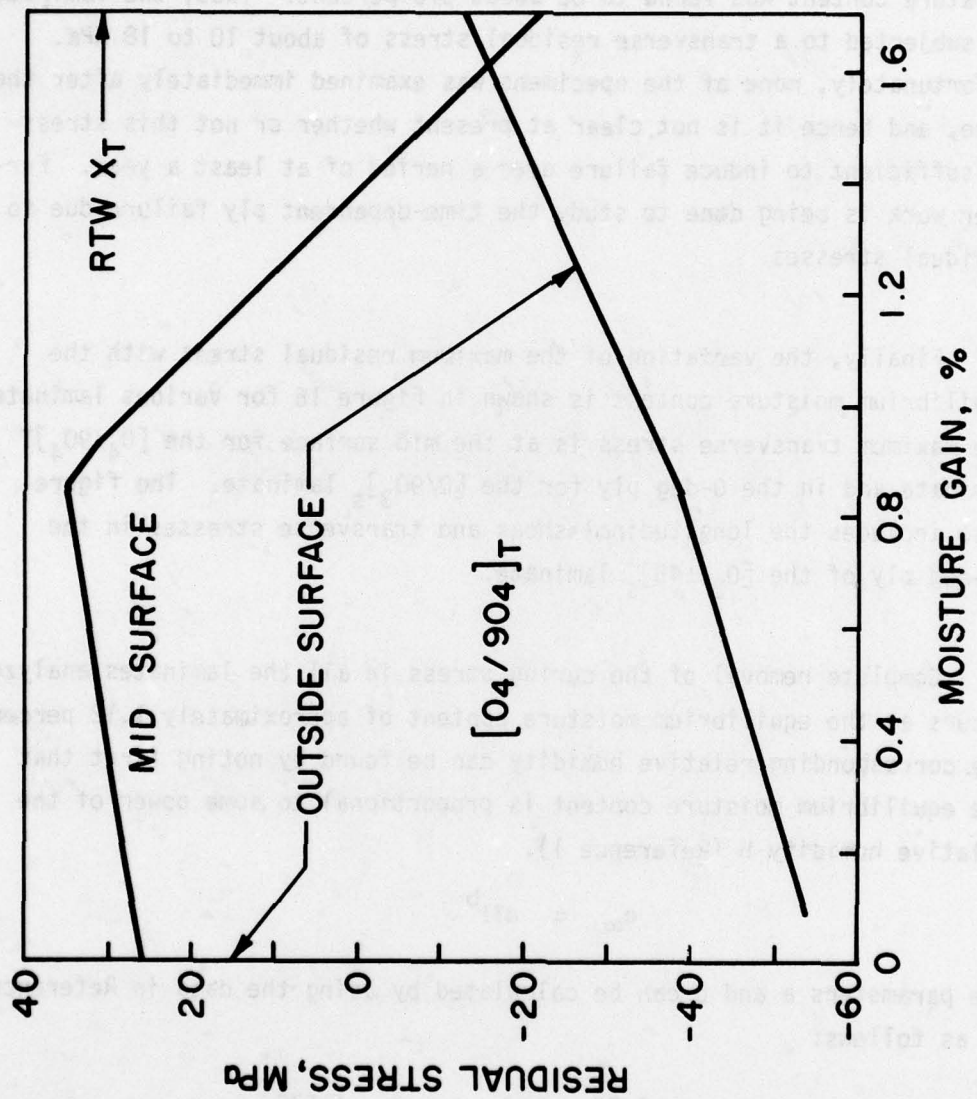Figure 12.   A Typical Crack in $[0_4/90_4]_T$ Laminate

Figure 13. Transverse Residual Stresses in $[0_4/90_4]_T$ Laminate During Absorption

Examination of Table 4 reveals that the various hygrothermal conditioning has little to do with the number of cracks. Figure 14 shows the transverse residual stresses at the room temperature as the equilibrium moisture content varies. The corresponding warpage is seen to agree well with the prediction in Figure 15. In the room environment the equilibrium moisture content was found to be about 0.6 percent. Thus, the laminate is subjected to a transverse residual stress of about 10 to 18 MPa. Unfortunately, none of the specimens was examined immediately after the cure, and hence it is not clear at present whether or not this stress is sufficient to induce failure over a period of at least a year. Further work is being done to study the time-dependent ply failure due to residual stresses.

Finally, the variation of the maximum residual stress with the equilibrium moisture content is shown in Figure 16 for various laminates. The maximum transverse stress is at the mid surface for the $[0_4/90_4]T$ laminate and in the 0-deg ply for the $[0/90_3]_s$ laminate. The figure also includes the longitudinal shear and transverse stresses in the 45-deg ply of the $[0_2/\pm45]_s$ laminate.

Complete removal of the curing stress in all the laminates analyzed occurs at the equilibrium moisture content of approximately 1.12 percent. The corresponding relative humidity can be found by noting first that the equilibrium moisture content is proportional to some power of the relative humidity H (Reference 1).

$$c_\infty = aH^b$$

The parameters a and b can be calculated by using the data in Reference 3, as follows:

$$a = 1.7\% \quad \text{and} \quad b = 1.675$$

Thus, the relative humidity at which no residual stress is present at 27^oC is
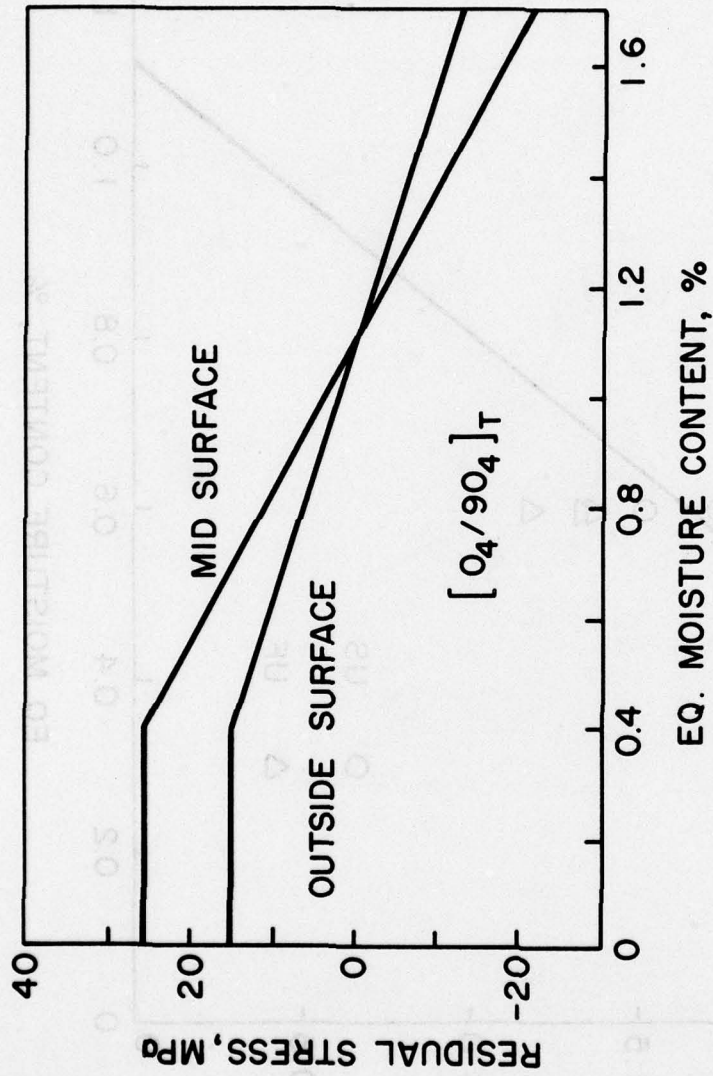
$$H = 78\%$$

36

Figure 14. Transverse Residual Stresses Versus Equilibrium Moisture Content for $[0_4/90_4]$ Laminates
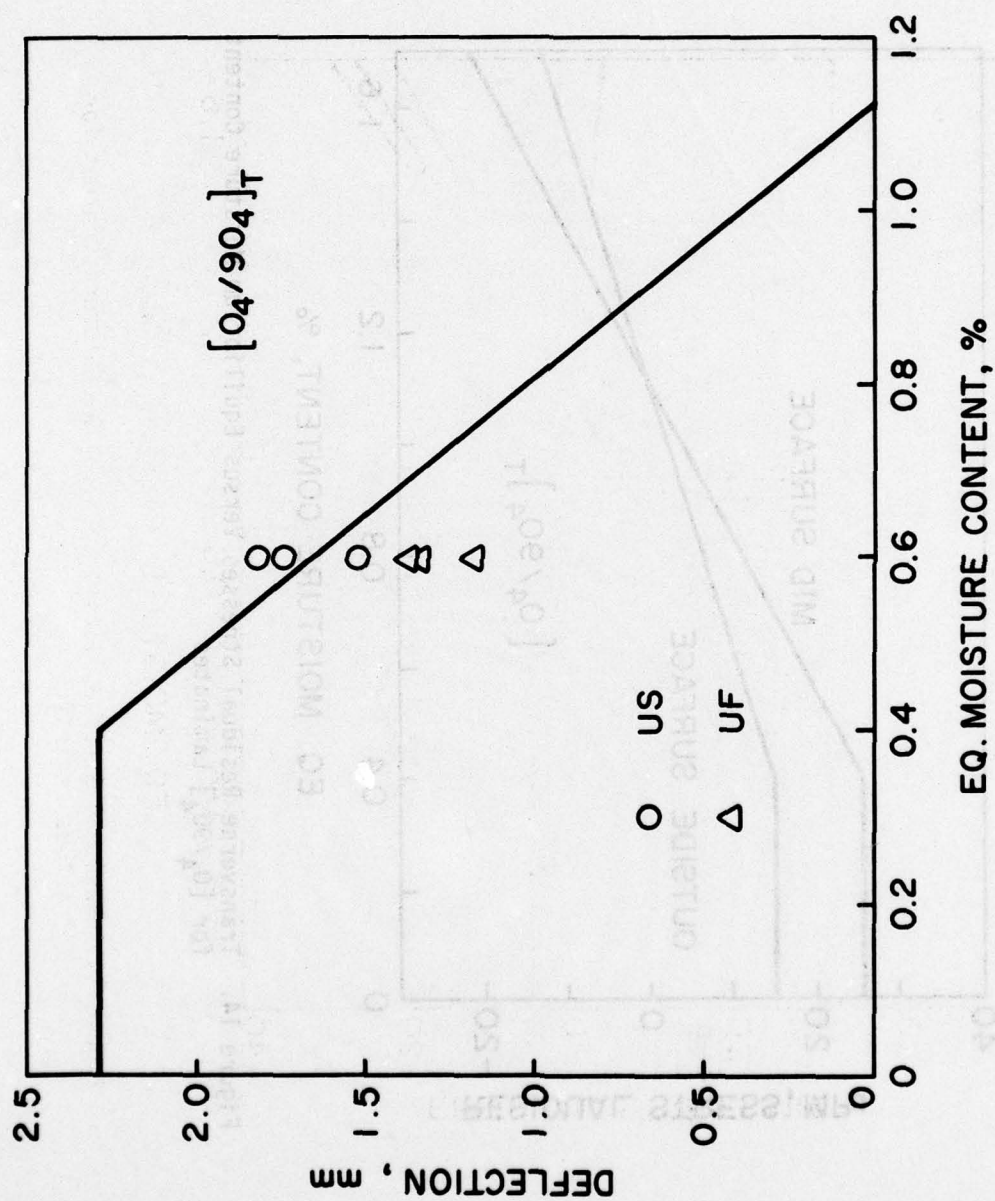
Figure 15.   Deflection Versus Equilibrium Moisture Content for $[0_4/90_4]$ Laminate
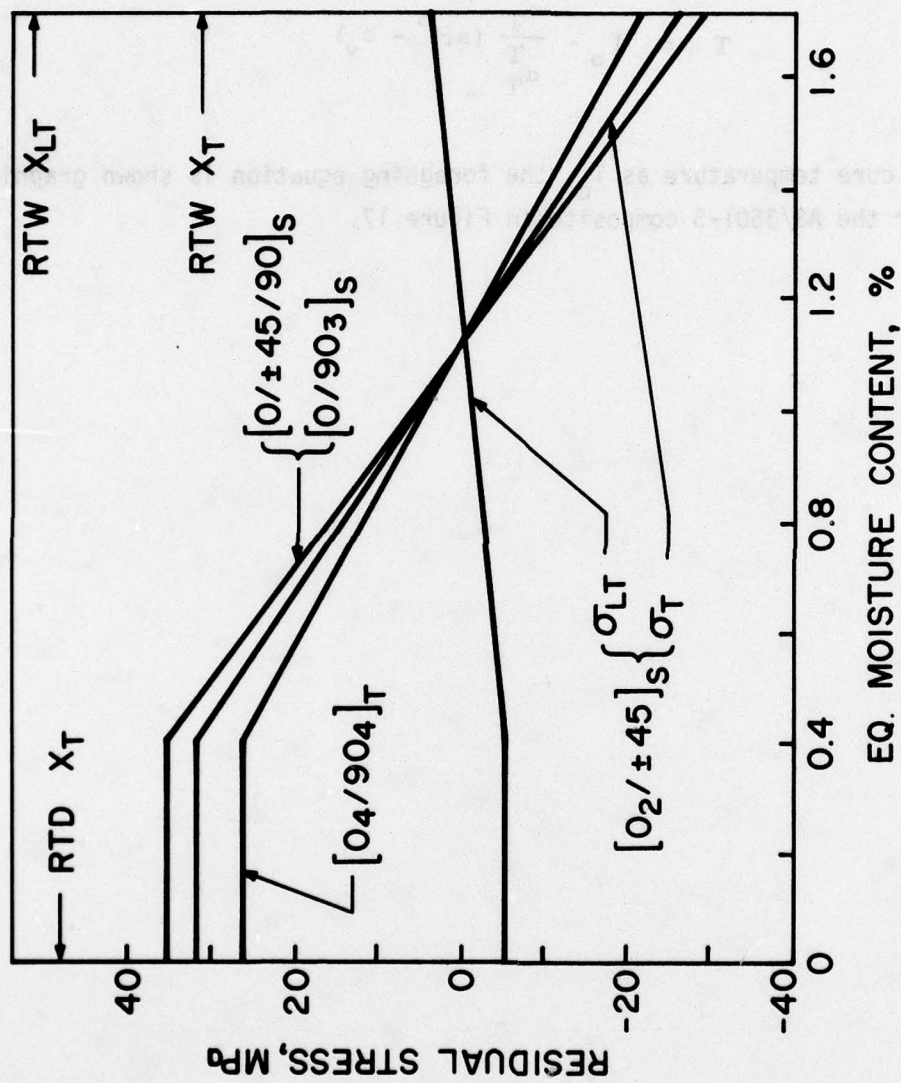
38

Figure 16. Residual Stresses Versus Equilibrium Moisture Content for Various Laminates

In fact, a simple relationship between the temperature and the relative humidity for the residual stress-free state can be obtained if α_L^T is neglected. In terms of the curing stress-free temperature T_o, the relationship becomes

$$T = T_o - \frac{\alpha_T^H}{\alpha_T^T} (aH^b - c_v)$$

With the cure temperature as T_o, the foregoing equation is shown graphically for the AS/3501-5 composite in Figure 17.

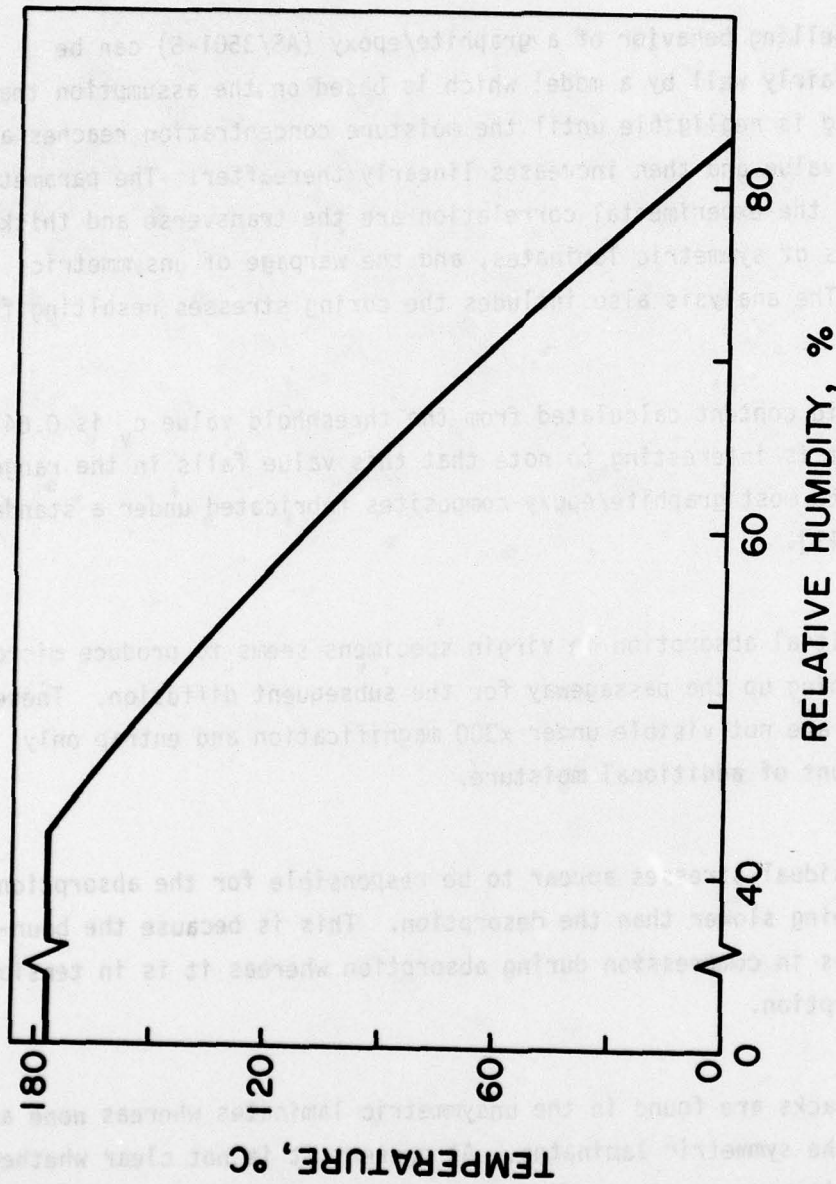40

TEMPERATURE, °C
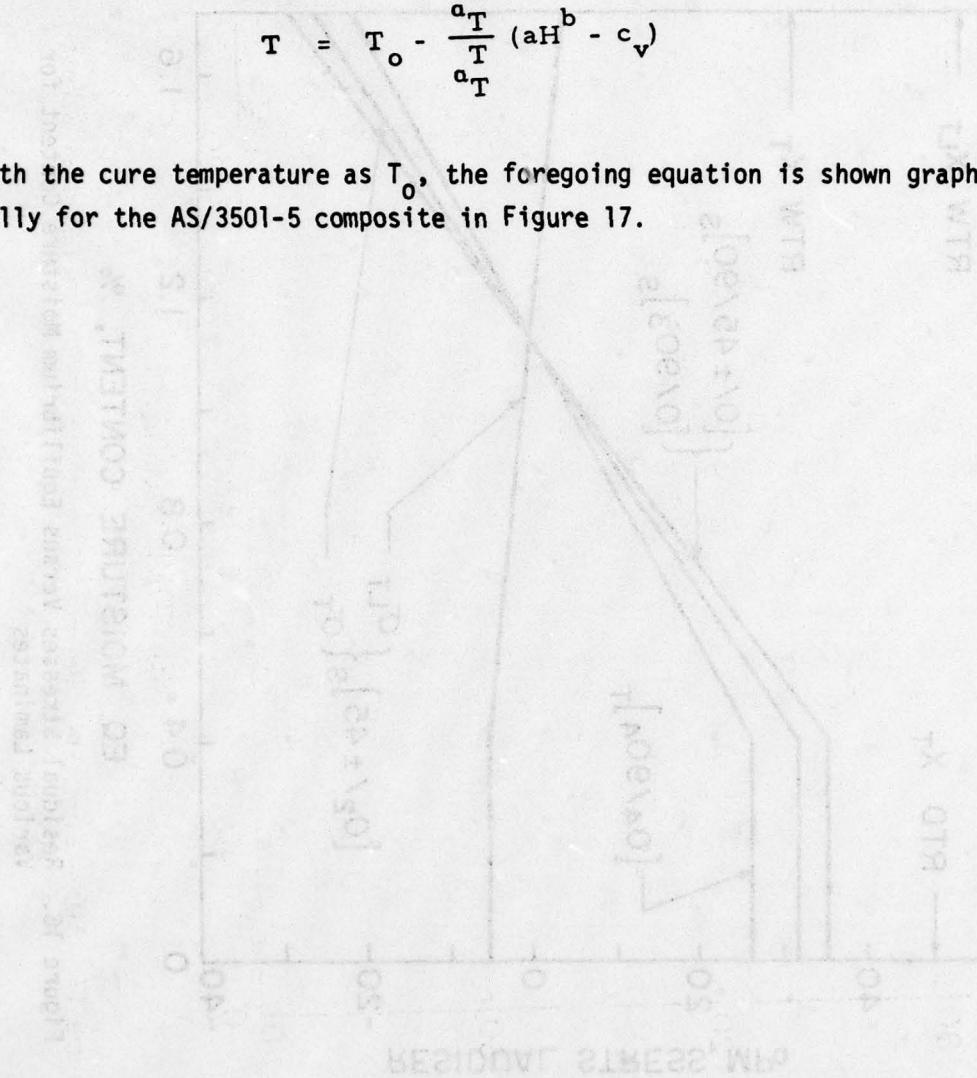
RELATIVE HUMIDITY, %

Figure 17. Temperature-Relative Humidity Relationship for Residual Stress-Free State

SECTION IV

CONCLUSIONS

The swelling behavior of a graphite/epoxy (AS/3501-5) can be described fairly well by a model which is based on the assumption that the swelling is negligible until the moisture concentration reaches a threshhold value and then increases linearly thereafter. The parameters involved in the experimental correlation are the transverse and thickness strains of symmetric laminates, and the warpage of unsymmetric laminate. The analysis also includes the curing stresses resulting from fabrication.

The void content calculated from the threshhold value c_v is 0.64 percent. It is interesting to note that this value falls in the range applicable to most graphite/epoxy composites fabricated under a standard procedure [11].

The initial absorption in virgin specimens seems to produce microcracks, opening up the passageway for the subsequent diffusion. These microcracks are not visible under x300 magnification and entrap only a small amount of additional moisture.

The residual stresses appear to be responsible for the absorption initially being slower than the desorption. This is because the boundary layer is in compression during absorption whereas it is in tension during desorption.

Many cracks are found in the unsymmetric laminates whereas none are present in the symmetric laminates. At present it is not clear whether or not this is because of any difference between AS/3501-5 and AS/3501-5A. In any case, the processing parameters such as cool-down rate, post cure temperature, and temperature distribution may affect the state of residual stress.

Since the present study is only a first step toward understanding the residual stresses and internal damages, the material behavior has been idealized as elastic, and any coupling between moisture and temperature has been neglected.   Therefore, improved models may be required to analyze the material response under complex environmental exposures. For example, the effects of thermal spiking (Reference 12) may necessitate the development of moisture-temperature-dependent viscoelastic models.

REFERENCES

1. C. H. Shen, and G. S. Springer, Journal of Composite Materials, Vol. 10, No. 1, 1976, pp. 2-20.

2. C. H. Shen, and G. S. Springer, Journal of Composite Materials, Vol. 11, No. 1, 1977, pp. 2-16.

3. C. E. Browning, G. E. Husman, and J. M. Whitney, in Composite Materials: Testing and Design (Fourth Conference), ASTM STP 617 American Society for Testing and Materials, 1977, pp. 481-496.

4. C. D. Shirrell, and J. Halpin, in Composite Materials: Testing and Design (Fourth Conference), ASTM STP 617, American Society for Testing and Materials, 1977, pp. 514-528.

5. H. T. Hahn, Journal of Composite Materials, Vol. 10, No. 4, 1976, pp. 266-278.

6. S. W. Tsai, and H. T. Hahn, Composite Materials Workbook, AFML-TR-77-33, Air Force Materials Laboratory, 1977.

7. N. J. Pagano, in Composite Materials, Vol 2, Mechanics of Composite Materials, G. P. Sendeckyj, Ed., Academic Press, New York, 1974, Chapter 2, pp. 23-44.

8. J. Crank, The Mathematics of Diffusion, Clarendon Press, Oxford, 1975

9. K. H. G. Ashbee, and N. Farrar, in Proc. of the 1975 Int'l Conf. on Composite Materials, The Matallurgical Soc. of AIME, 1976, pp. 771-782.

10. G. S. Park, in Diffusion in Polymers, J. Crank and G. S. Park, Eds., Academic Press, London, 1968, Chapter 5, pp. 141-163.

11. J. C. Halpin, An Assessment of Life Assurance Methodology for Advanced Composite Structures, presented at the 18th Joint AIAA/ASME Structures and Structural Dynamics Meeting, San Diego, March 21-23, 1977.

12. E. L. McKague, Jr., J. E. Halkias, and J. D. Reynolds, Journal of Composite Materials, Vol. 9, No. 1, 1975, pp. 2-9